PHYSICAL REVIEW B VOLUME 19, NUMBER 6 15 MARCH 1979

Oxygen monolayers adsorbed on graphite studied by neutron scattering

Mourits Nielsen
Risø National Laboratory, DK-4000 Roskilde, Denmark

John P. McTague
University of California, Los Angeles, California 90024
(Received 13 November 1978)

The phase diagram of absorbed films of O_2 molecules on (002) surfaces of graphite has been measured in the range of densities from submonolayer to 1.6 monolayer. This system is particularly interesting because it orders magnetically below 11.9 K for dense monolayer and higher coverages. This magnetic order is observed both through the antiferromagnetic-superstructure-Bragg reflection as well as through the accompanying magnetostrictive distortion which is seen as a splitting of the nuclear Bragg scattering peak. In all, three distinct two-dimensionally ordered phases have been found, each being incommensurate with the graphite surface lattice. Both first-order and continuous transitions have been observed between these phases.

I. INTRODUCTION

The condensed phases of molecular oxygen O_2 are unusual in that the O_2 molecule has two unpaired electrons in a triplet $S=1$ state, and the spins on neighboring molecules interact via a direct overlap coupling. Its low-temperature α phase is the only known direct overlap homonuclear antiferromagnet, and exhibits a strong magnetoelastic distortion.[1] At higher temperatures the paramagnetic β phase is undistorted on average, and the bulk α-β transition is of first order.[2]

It is of particular interest to investigate the structure and phase transitions of this simple antiferromagnet in two dimensions. Recent studies of physisorbed rare-gas layers on uniform surfaces have shown that many of their properties are essentially two dimensional (2D) in character.[3] Structural probes such as low-energy electron diffraction (LEED)[4] and neutron diffraction[5] have observed and identified a variety of phases in these thin films, and there have even been a few neutron measurements of their dynamics.[3,5] The nature of the phase transitions in these systems has attracted both experimental[4,6,7] and theoretical interest.[8]

We report here neutron-diffraction measurements of both the structural and magnetic properties of O_2 physisorbed on Grafoil,[9] a uniform graphite material with large specific surface area consisting predominantly of (001) planes. Grafoil has nearly ideal properties for the study of adsorbed thin films by both thermodynamic and structural probes, among which neutron scattering is one of the most powerful and direct. Although it is not a surface-specific probe, recent measurements on such diverse adsorbed substances as N_2, ^{36}Ar, Kr, H_2, D_2, ^4He, ^3He, and CH_4 have established the applicability of the neutron technique even to submonolayer coverages of coherent scatterers, and each species investigated has revealed new structural or dynamic behavior.[3]

O_2 molecules have only a small molecular electrical quadrupole moment, so they tend to align alongside each other in condensed phases with their magnetic moments confined to the plane perpendicular to the molecular axis. As a result, the bulk α phase consists of sheets of molecules very tightly packed in a distorted triangular structure, with their molecular axes normal to the plane and an antiferromagnetic planar structure. It is natural then to inquire whether analogous structural and magnetic order occurs in monolayer films. The results described below confirm the existence of such a phase, in addition to two other distinct monolayer phases. Aspects of the thin-film phase diagram and phase transitions are also reported. A preliminary report on these measurements was published earlier.[10]

II. SAMPLE

It was first discovered in thermodynamic measurements[11] on monolayers, that the Grafoil substrate gives very distinct phase diagrams, proving that the adsorbing surfaces must be of highly homogeneous quality. Diffraction techniques using, e.g., neutrons, x-rays, or low-energy electrons reveal such properties of the substrate as the effective coherence size of the adsorbing surfaces and their crystallographic orientation, while direct observation by electromicrography shows that Grafoil consists of grains of single crystalline graphite which have large surfaces parallel to the hexagonal planes of the crystal of dimension 1–10 μm. This is sketched in Fig. 1. There is some uncertainty about the typical thickness of the

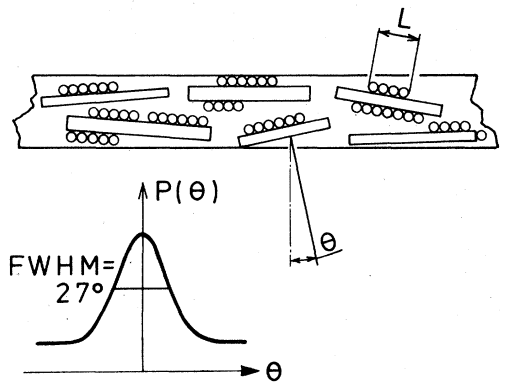

FIG. 1. Schematic drawing of Grafoil sheet. L indicates the typical coherence length of the adsorbed layers. $P(\theta)$ describes the distribution of angles giving the nonparallelism of the substrate surfaces.

grains. From the width of neutron Bragg peaks one estimates a coherence thickness of about 100 Å, whereas a calculation using the measured total area gives a geometric thickness of 300 Å. The 2D homogeneity of the surfaces is likewise restricted, presumably by steps in the atomic layers and other crystal faults. From the shape of the observed Bragg reflection from the adsorbed layers, one can deduce that the maximum coherence length L of the crystalline ordered adsorbed layers is in the range of 100–150 Å (see Fig. 1).

The total area for adsorption of the sample used here is 28 m^2 per gram as determined both from vapor pressure isotherms and from diffraction measurements. In the individual Grafoil sheets the adsorbing surfaces have a substantial degree of relative parallelism and are predominantly parallel to the macroscopic foil surface: rocking curves of the (002) Bragg reflection are Gaussian shaped with a full width of half-maximum (FWHM) of 27° (see Fig. 1). This property of the substrate allows a distinction in the spectroscopic measurements between properties parallel and perpendicular to the film plane.

The substrate is obtained as 0.2-mm-thick sheets, out of which we cut circular discs, 30 mm in diameter. These discs were baked out at 100 °C in vacuum and installed in the sample cell without being exposed to air. In the sample cell the discs are oriented horizontally, making them parallel to the neutron scattering plane. The total weight of Grafoil in the cell was 41.4 g. It was mounted in a He cryostat, and the O_2 gas was introduced through a capillary tube. The amount of gas adsorbed (referred to as the filling) was monitored at room temperature by measuring the gas pressure in a 2-liter bulb from which the O_2 gas was added to or subtracted from the sample cell. Each time the filling was changed the temperature of the sample cell was raised to about 70 °K. Subsequent cooling to low temperature took place over 3–4 h intervals, which was determined to be sufficiently slow to allow for surface phase annealing.

III. NEUTRON SCATTERING TECHNIQUE

The measurements were performed on triple-axis spectrometers. For small momentum transfers we used the cold source beam and an energy of 4.7 meV. A considerable reduction of the background scattering from the substrate is obtained by using neutron energies E near or below the cutoff of Bragg reflections from the basal plane points of the reciprocal lattice of graphite, i.e., the (hk0) reflections, occurring at $E = 4.5$ meV. The main source of the background is multiple scattering in which the neutrons are scattered two or more times in the sample. Lowering the energy to 4.7 meV reduces the number of possible scattering processes involving (hk0) reflections to the extent that the remaining background is due to other sources. All measurements were done with the analyzer set to accept only the elastically scattered neutrons, which further optimized the signal to background ratio.

IV. DETERMINATION OF THE PHASE DIAGRAM OF THE TWO-DIMENSIONAL MOLECULAR LATTICES

A. Shape of the diffraction peaks

For an ordered monolayer there is no limitation in the Bragg condition on the momentum transfer perpendicular to the film. Nevertheless, a single ordered film oriented at a given angle to the neutron scattering plane would give sharp Bragg peaks as with three-dimensional crystals. However, in the case of adsorbed layers on Grafoil two kinds of disorder change the diffraction pattern. First, there is no correlation between the angles with which the individually adsorbed films are rotated around their normal vector. The layers thus constitute a 2D powder. This means that scattering points for a set of films all parallel to the scattering plane are in two dimensions located on circles with radii equal to the length of the 2D reciprocal-lattice vector and in three dimensions on cylinders. The second kind of disorder of the adsorbed films is constituted by the nonparallelism of the layers, because the c axes of the graphite crystals are distributed in a 27° FWHM range around the ideal orientation (see Fig. 1). Consequently, the Bragg peaks from ordered layers on Grafoil are distorted. A layer whose normal vector is tilted an angle θ towards the neutron scattering

vector Q will contribute to the Bragg scattering when $Q = \tau_0/\cos\theta$. With all orientations taken into account, we then get the following line shape:

$$[I(Q)]_{\tau,L,w} = AI_0 \int_0^{\pi/2} \int_0^{Q} e^{-\theta^2/w^2} \times e^{-(\tau-\tau_0)^2/\Delta^2} (Q\sqrt{Q^2-\tau^2})^{-1} d\psi d\tau, \quad (1)$$

where A is a normalizing factor, I_0 the integrated intensity, τ_0 is the reciprocal-lattice vector of the 2D structure, and $\Delta \equiv 2\sqrt{\pi}/L$, where L is the coherence length. The factor $e^{-(\theta/w)^2}$ is a weighting function describing the nonparallelism of the adsorbing surfaces. The width of the distribution function is measured by diffraction to be $w = 16°$. Finally, $\cos\theta = \tau/Q\cos\psi$. The resultant line shape is a rounded saw tooth with a steep edge on the low Q side, determined predominantly by L, and a high Q tail which is essentially controlled by w.

The line-shape formula of Eq. (1) is modified by a form factor if the 2D unit cell contains more than one atom. For an O_2 molecule oriented perpendicular to the graphite surface this has the value $\cos^2(\frac{1}{2}Qd\sin\theta)$, where θ is the angle at which the graphite surface is tilted relative to the scattering plane. Finally, molecular translational, librational, and vibrational motion may be accounted for by a Debye-Waller factor, whose variation is significant only when comparing the relative intensities of different Bragg peaks. The effect of tilt distribution and molecular form factor are shown and compared to an observed (10) profile in Fig. 2. An improvement in the fitting of the

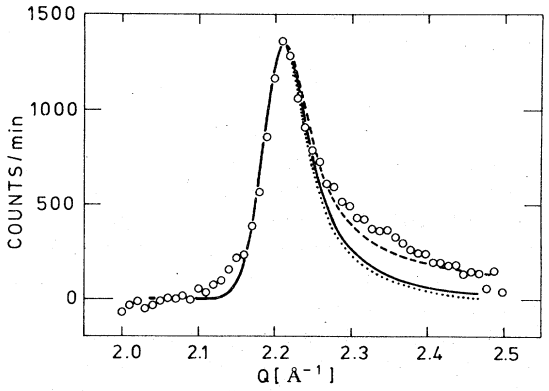

FIG. 2. Observed (10) Bragg reflection from an O_2 layer forming an even lateral triangular structure. The circles are the measured intensities after subtraction of the scattering from the substrate. The coverage is $\rho = 1.83$ and $T = 26$ K. The observed intensity is fitted to the line shape, formula 1. For the full line the parameters are $\omega = 16°$, $L = 105$ Å and $\tau(10) = 2.2$ Å^{-1}. The dotted curve has the same parameters but a molecular form factor has been included. The curve with the broken line giving the best fit has the same parameters again, but an isotropic angular distribution has been added to the Gaussian distribution, $P(\theta) = 0.3 + e^{-\theta^2/w^2}$.

curve is obtained by adding an isotropic distribution to the Gaussian distribution for the tilt angle so that $P(\theta) = H_0 + H_1 \times e^{-\theta^2/w^2}$. We have used the same values of H_0/H_1 as Kjems *et al.*[12]

B. Phase diagram

By measuring the diffraction peaks from the adsorbed O_2 layer for various fillings and temperature we arrive at the coverage-temperature phase diagram shown in Fig. 3.

The amount of gas which is adsorbed in the sample cell and which is referred to as the filling is reported in units of that amount which would just complete a monolayer having the particular monolayer structure usually called the $\sqrt{3}\times\sqrt{3}$ structure.[12] Here an atom or a molecule is located on every third hexagon of the hexagonal surface planes of graphite crystals. This structure is not found for adsorbed O_2 layers but is used to define the unit because it has a distinct 2D density and occurs for several other adsorbed gases. The amount of gas which is equivalent to $\rho = 1$ was determined in a previous measurement on adsorbed H_2 and D_2 on Grafoil[13] using the same sample cell and it equals 277 cm^3 STP.

δ phase

In the phase diagram of Fig. 3 the phase δ is observed for $\rho < 1.68$ and for temperatures lower than indicated by the melting line. Figure 4 shows a series of diffraction groups for different coverages in this range at $T = 4.2$ K. In all cases the scattering from the substrate has been subtracted. The full lines are fitted curves using formula (1), where the intensity I_0, the position τ_0, and the coherence length L have been varied. Most weight is given the points along the leading left-hand front of the group in order to find the best values of τ_0

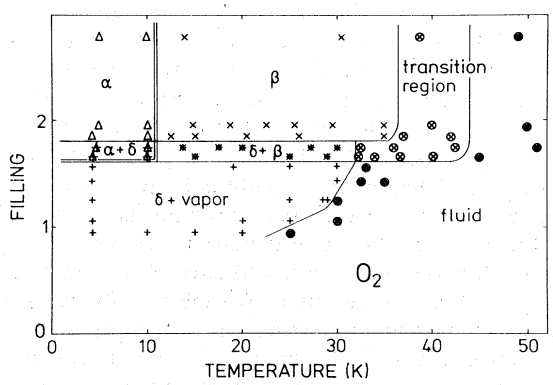

FIG. 3. Phase diagram of adsorbed O_2 layers. The filling is measured in units of the gas amount needed to complete a commensurate $\sqrt{3}$ structure. The points show where diffraction groups have been observed.

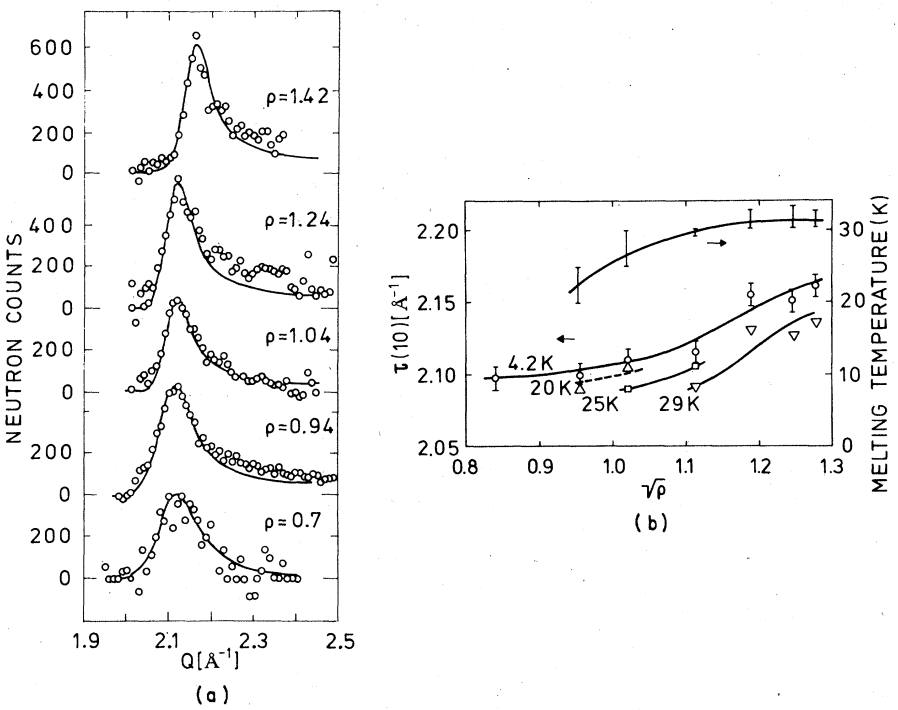

FIG. 4. (a) Neutron-diffraction groups observed from O_2 monolayers in the δ phase. The circles are the observed intensities corrected for the scattering from the substrate. The curves are the fitted line shapes. (b) Length of the (10) reciprocal-lattice vector obtained by fitting the curves in Fig. 4(a) and plotted vs the square root of the coverage ρ. The upper curve shows the melting temperature vs $\sqrt{\rho}$. The lines are guides to the eye.

and L. The position of the Bragg peak and the fact that no other scattering peak from the film is found in the region from 1.6 $Å^{-1}$ to 2.8 $Å^{-1}$ show that the monolayer must have an equilateral triangular structure and the observed Bragg peak is the (10) reflection. Any other possible structure would give additional Bragg-peaks in the range investigated. There is no registry between the O_2 and the substrate structure.

Figure 4 also shows the variation of τ_0 with filling and temperature. The packing of oxygen molecules in bulk solid O_2 has been discussed by Barrett and Meyer,[2] who used calculated molecular electron density contours to estimate how densely the molecules can be packed. The resultant length and thickness are 4.18 and 3.1 Å, respectively. In the O_2 layers on Grafoil the nearest-neighbor distance a_{nn} varies in the δ phase between 3.37 and 3.47 Å. We can then conclude that the molecules cannot have the molecular axis parallel with the substrate, because they would not have sufficient space to be free rotors parallel with the substrate, and if they were forming domains with parallel molecular axis then we would have observed more than one Bragg reflection. We infer, rather, that the molecules form an even lateral triangular structure where the averaged tilt angle between the molecular axis and the normal to the substrate probably varies with the value of a_{nn}. If we use the same molecular model as Barrett and Meyer, then the average tilt angle can be as large as 40° for the the O_2 molecules in the δ phase.

As the temperature is raised through the melting region between the δ phase and the fluid phase the Bragg peak intensity goes to zero in a continuous fashion. Ar has also been found to form noncommensurate monolayers which both experimentally[14] and in molecular dynamics calculations[15] have been found to have a continuous melting transition. In the fluid phase the order is so small that no neutron diffraction has been identified.

α and β phase

When the filling is increased at low temperature the Bragg peak splits into a double peak signalling a distortion of the triangular lattice. This sets in at $\rho \geq 1.61$ and coincides with the completion of a monolayer of the δ phase. The region of ρ and T in which the splitting is observed is indicated in Fig. 3 as the α phase.

These Bragg peaks strongly suggest that the O_2 layers have the same structures as the densest packed planes of bulk solid α O_2. In the bulk phase the molecular axis is oriented perpendicular to the planes, and the centers of the molecules are located on a skew triangular lattice, as shown in Fig. 5. When the temperature of O_2 layers in this phase is increased the splitting of the Bragg peak disappears around 11.9 K, and all the scattering intensity is then contained in a single peak, giving a good fit to the calculated line shape (see Fig. 6). The single Bragg peak observed above 11.9 K in the β phase shows that in this phase the monolay-

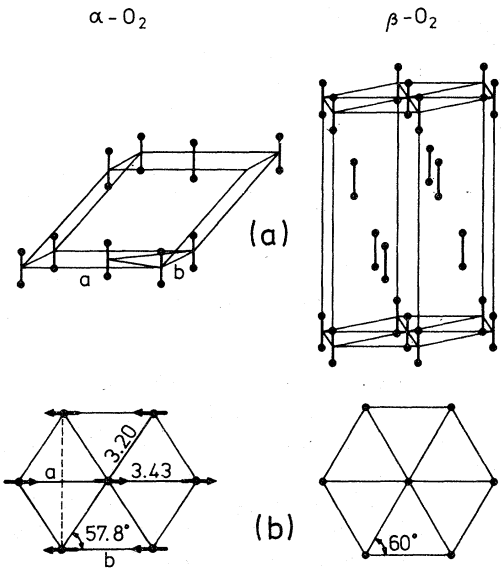

FIG. 5. (a) Structure of bulk α and β O_2. (b) Structures of the densest packed planes of bulk α and β O_2.

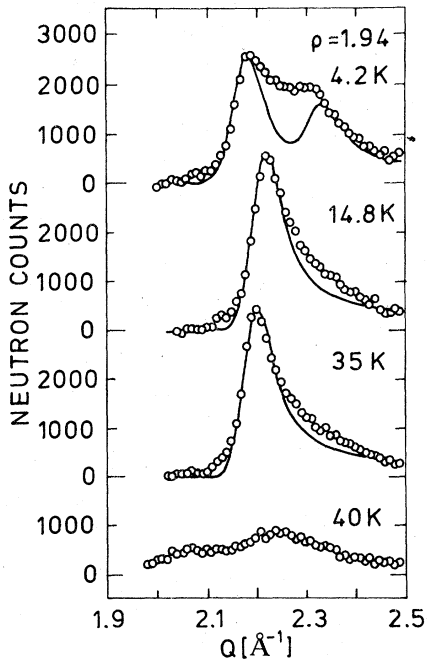

FIG. 6. Neutron-diffraction groups observed from O_2 layers in the α and β phase. The filling is $\rho = 1.94$ and the temperatures are given in the figure. The circles are measured intensities corrected for the scattering from the substrate, and the curves are the calculated line shapes assuming that the lattice parameters are those of densest packed planes of bulk O_2, in the α and β phase. The amplitude of the groups is obtained by fitting the amplitude of β-phase groups to the observed points.

ers have a structure which within our measuring accuracy, is identical to the basal plane structure of bulk β O_2 shown in Fig. 5.

We have calculated the shape of the diffraction peaks from the O_2 layers assuming that they have structures identical to the basal plane structures of the bulk O_2, and this is shown in Fig. 6. The intensity has been adjusted to match the β-phase group, but otherwise no parameter is varied. Note that the intensity of the high-Q peak of the α phase is half of that of the low-Q peak in agreement with the proposed structure (see Fig. 5).

When the filling is increased well beyond $\rho = 1.61$, the second layer contributes significantly to the scattering group of the α phase. This is seen in Fig. 7, where the measured Bragg peaks at different values of ρ are shown. The molecules of the second layer must be adsorbed in positions which are in registry with the first layer since a rather strong variation of the scattering profile is observed. Although the positions of the second-lay-

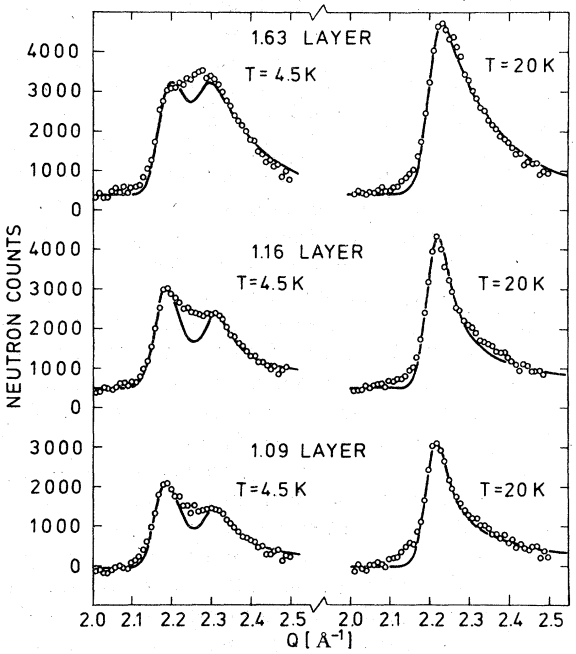

FIG. 7. Neutron-diffraction groups from O_2 layers of three different fillings with partial second-layer occupancy as shown in the figure. The density of the first layer is determined by the diffraction peaks. The substrate scattering is subtracted. The full lines are fitted curves where it is assumed that the second-layer molecules are adsorbed in registered positions above the center of the triangles of the first adsorbed O_2 layer. At each filling the fitting parameters for the 20-K group was the length of the $\tau(10)$ vector, the peak intensity and a correcting background. In the fitting of the 4.5-K group the same values of the peak intensity and the correcting background was used. The values of the τ vectors are given in Table I.

TABLE I. Lattice vectors given by the curves in Fig. 7.

Filling	1.84	1.94	2.74 ± 0.01
Number of layers	1.09	1.16	1.63
Reciprocal-lattice vectors at $T=4.5$ K (Å^{-1})	2.170	2.170	2.175 ± 0.005
	2.30	2.30	2.28 ± 0.02
Nearest-neighbor distances a_{nn} at $T=4.5$ K (Å)	3.22	3.22	3.23
	3.41	3.41	3.39
Reciprocal-lattice vectors at $T=20$ K (Å^{-1})	2.203	2.203	2.205 ± 0.005
Nearest-neighbor distances a_{nn} at $T=20$ K (Å)	3.293	3.293	3.290

er molecules or their rotational orientation cannot be determined from the present results, the observed line shape sets conditions on possible location.

In cases where second-layer particles are located in registry with and exactly above the first layer particles, the two layers will, in a diffraction experiment, scatter in phase for substrate surfaces with tilt angle zero, and the resulting scattering profile will sharpen up as a result of the scattering from the second layer. If, on the other hand, the second-layer particles are located above the centers of the triangles of the first layer structure, then we will get extra scattering on the high-Q side of the Bragg scattering profile, and agreement with our observed profiles is obtained using this assumption as shown in Fig. 7. We have fitted the position of the Bragg peaks, and those values are given in Table I together with the corresponding nearest-neighbor distances. The two values of a_{nn} correspond to the nearest-neighbor distances 3.20 and 3.43 Å in Fig. 5. The second-layer molecules are assumed to be 3.75 Å above the first layer, the same as in solid bulk α O_2.[2] For each of the three coverages a peak intensity and a correcting background is determined by fitting to the curves at 20 K, and the same values are used in calculating the curves at 4.5 K.

When the temperature is increased in the β phase the Bragg scattering intensity decreases and the groups get broader. This happens in a 7–10-K broad temperature range, and this is denoted as the "transition region" in Fig. 4. There is no sharp signature in our data which defines this region, but it is included in the diagram to signify that the "melting" occurs over a broad temperature range.

Coexistence regions

Between the δ and the α or β phases in Fig. 3 there are coexistence regimes. Figure 8 shows a series of scans at constant filling at points through the $\delta+\alpha$, $\delta+\beta$, and the transition region of the phase diagram. Although the $\delta+\alpha$ coexistence is not obvious in this figure, it appears clearly on spectra obtained using ZYX, a better oriented graphite substrate (see below). In the $\delta+\beta$ region two maxima are observed, whose positions coincide with the positions of the Bragg peaks of the δ and β phases. At different fillings ρ in this coexistence region, the relative intensity of the two peaks varies according to the expected ratio of molecules going into the two phases.

From the measured position of the Bragg peaks we can calculate the respective fillings for monolayer completion. Near completion of the δ phase we find $\tau(10)=2.15$ Å^{-1}. The commensurate $\sqrt{3}$ structure has $\tau(10)=1.703$ Å^{-1}, and thus we get $\rho=1.59$ at the δ-phase monolayer completion. For

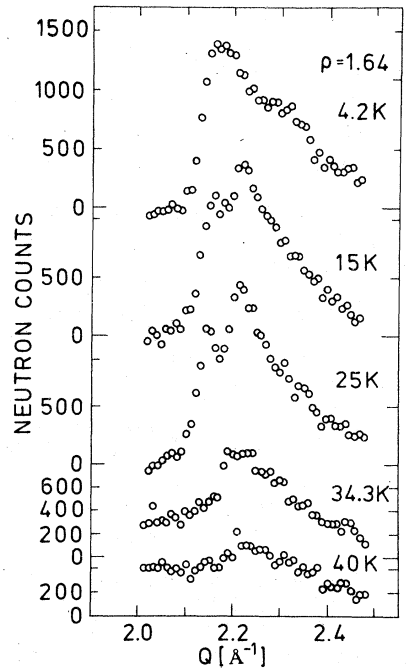

FIG. 8. Neutron-diffraction groups observed in the $\alpha+\delta$, $\beta+\delta$, and the transition region. The filling is $\rho=1.64$ and the various temperatures are given in the figure. The intensities are corrected for the substrate scattering.

TABLE II. Phase-diagram data.

	$\tau(10)$ (Å^{-1})	ρ	a_{nn} (Å)
At completion of δ phase	2.15 ± 0.01	1.59 ± 0.01	3.37
At phase boundary between δ and $\delta+\beta$		1.61 ± 0.02	
At completion of α phase monolayer	2.170 ± 0.005 2.30 ± 0.02	1.69 ± 0.01	3.41 3.22
At completion of β phase monolayer (15 K)	2.210 ± 0.005	1.69 ± 0.01	3.28
At phase boundary between $\delta+\beta$ and β		1.76 ± 0.02	

the β and the α phases we find similarly that monolayer completion corresponds to $\rho = 1.69$. The phase lines in the diagram of Fig. 3 were determined by using the actual amount of gas and the known total area for adsorption. The more accurate values of ρ which delimit the $\delta+\beta$ coexistence region were obtained with help of the relative intensities of the δ and the β component of the diffraction groups, and these values are given in Table II. The lower limit coincides very closely with the completion of the δ-phase monolayer. Since the upper limit lies about 4% above the β-phase monolayer completion, a few per cent occupancy of molecules in the second layer appears needed for the first layer to assume the pure β phase. Second-layer particles give rise to an effective pressure within the first layer. The limits of the $\delta+\alpha$ to the pure α phase have not been observed, but in diffraction scans where the ZYX substrate was used (see below) it was found that a coexisting δ component of the Bragg scattering group does not change intensity when we go through the $\alpha+\delta$ to $\beta+\delta$ phase transition. Thus we conclude that for a given value of ρ the same fraction of the adsorbed layer has the δ phase in the $\alpha+\delta$ coexistence region as in the $\beta+\delta$ one.

When entering the transition region from the $\beta+\delta$ phase the δ-phase component of the double Bragg peak disappears, and at further increasing temperature the other component associated with the β phase decreases in intensity. The details of the phase diagram in that part of Fig. 3 where β, $\delta+\beta$, δ, and transition region joins, cannot be determined from the present data.

Magnetic ordering and the α-β phase transition

One of the objectives of these measurements was to investigate possible ordering of the magnetic moments of the O_2 molecules. The very close analogy which exists between the nuclear structures of the adsorbed layers and the bulk structures was indeed found also to apply to the magnetic properties. From the spin ordering of the basal planes of bulk solid O_2 sketched in Fig. 5 it may be seen that this causes a doubling of the magnetic unit cell in the $\vec{a}$ direction and gives rise to a magnetic Bragg peak at the position of half the momentum transfer of the high-Q component of the split nuclear Bragg peak of the α phase. Figure 9 shows the measured magnetic groups.

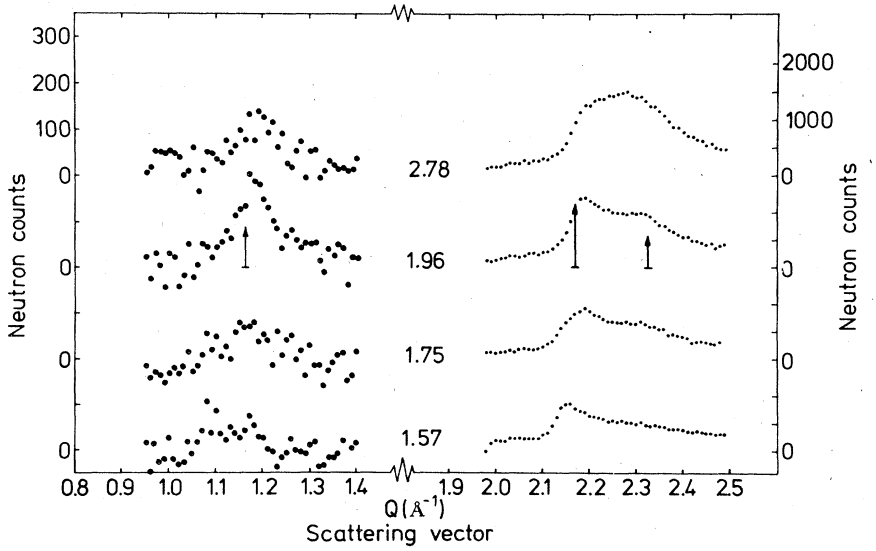

FIG. 9. Neutron-diffraction groups from O_2 layers at $T = 4.2$ K. The fillings ρ are given in the figure. Displayed on the right-hand side is the difference spectrum $[J(Q)]_{\text{Grafoil}+O_2} - [J(Q)]_{\text{Grafoil}}$, while the left-hand side is $J(Q, T = 4.2\text{ K}) - [J(Q, T = 20\text{ K})]_{\text{Grafoil}+O_2}$. The latter are the magnetic superlattic reflections. The three arrows indicate the positions and the relative intensities of diffraction peaks from O_2 monolayers identical to the densest packed planes of bulk O_2 in the α phase.

Only the $\rho = 1.96$ group is reasonably well resolved. The arrows in the figure, indicating positions and relative intensities of the groups, are calculated under the assumption that the structure is identical to the basal plane structure of the bulk O_2, with the intensity normalized to the low-Q component of the split nuclear group. In calculating the magnetic scattering intensity we have used the magnetic form factors given by Alicanov.[16] Even at fillings below $\rho = 1.61$ where we are within the δ phase, some magnetic scattering is observed near the positions of the magnetic Bragg peaks. The scattering is over a broad region of momentum but apparently centered at a little smaller Q than the group for $\rho = 1.96$. At high values of ρ ($\rho = 2.78$) approaching second-layer completion ($\rho = 3.38$) we observe, as discussed above, a double nuclear peak with a distorted line shape, signalling that molecules in the second layer are located in registry with the first layer. If we assume that the structure is the same as for the first layer but displaced as shown in Fig. 10, then the magnetic ordering in the second layer will influence the magnetic Bragg peak. The peak intensity will not change, but extra scattering intensity should be observed at the high-Q side of the peak. The scatter of the experimental points of the magnetic Bragg peaks in Fig. 9 does not allow an interpretation of the line shapes except that we notice broadening of the magnetic Bragg peak when second-layer molecules are present, consistent with the proposed structure.

The phase transition between the α phase and the β phase has been investigated both by measuring the nuclear and the magnetic Bragg peaks. In Fig. 11 the scattering intensity at the position of the maximum of the low-temperature magnetic Bragg peak, is shown as a function of temperature for both increasing and decreasing temperature cycles. The substrate scattering has not been subtracted; the count rate of 3200 in the figure corresponds to the substrate scattering. If the position of the Bragg peak changes with temperature then a part of the intensity variation can be caused by this. However, estimates indicate this effect to be insignificant. The variation of the magnetic Bragg intensity in Fig. 11 indicates that the α-β transition is continuous. Unfortunately, the weak magnetic scattering does not allow a more detailed study.

The structural aspects of the α-β transition are somewhat obscured by line broadening, due to the finite substrate coherence length L and to the orientational distribution of the Grafoil surfaces. In order to study these groups at the temperature of the α-β transition we have used another substrate called UCAR ZYX (Ref. 17), which was lent to us by Bretz. ZYX is a graphite which improved orientational and coherence properties but which, unfortunately, has only about $\frac{1}{10}$ the specific surface area, a severely limiting factor for neutron scattering studies. Preliminary neutron-diffraction data for a filling in the $\delta + \alpha$ coexistence region are shown in Fig. 12. The improved resolution allows clear identification of the low-Q δ-phase peak at all temperatures and shows the continuous collapse of the α-phase structural peak splitting as the temperature increases. We conjecture that this splitting is a magnetoelastic effect;

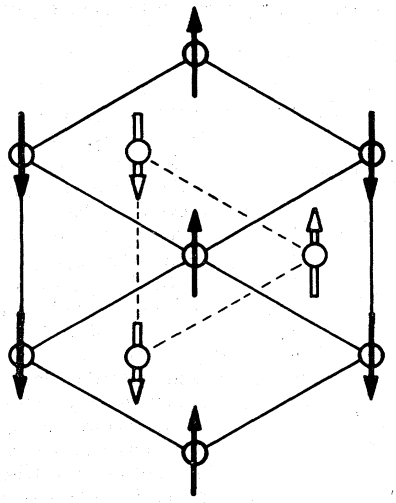

FIG. 10. Structure of the α phase. The open circles and arrows show the proposed structure of the second adsorbed layer of O_2 molecules.

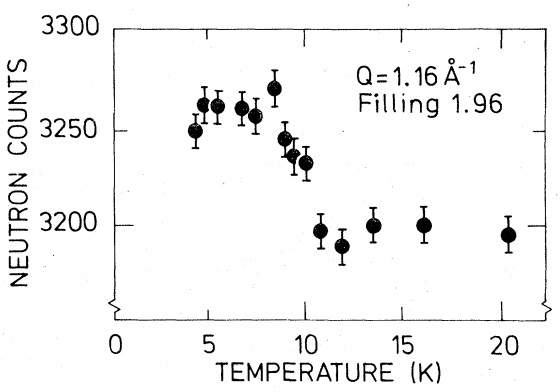

FIG. 11. Neutron scattering intensity at the position of the maximum of the magnetic superlattice reflection from adsorbed O_2 layers in the α phase. The coverage is $\rho = 1.96$ corresponding to 1.16 times a monolayer. The substrate scattering is not subtracted and it corresponds to the count rate 3200 in the figure.

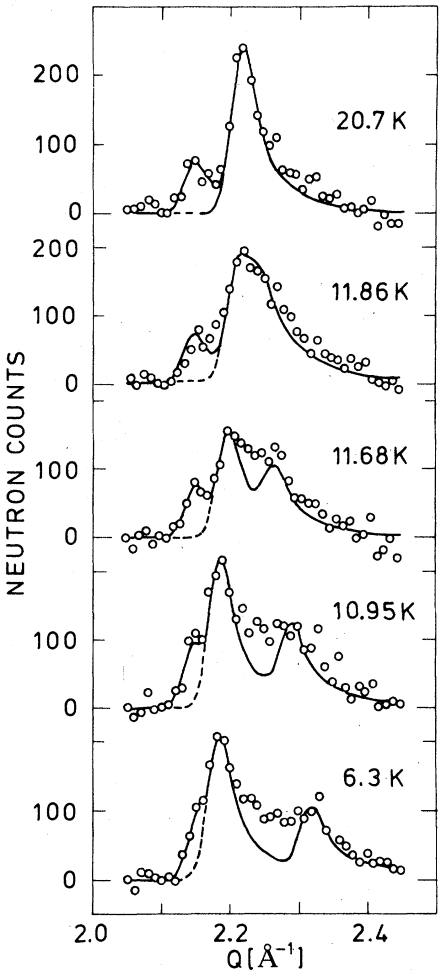

FIG. 12. Neutron-diffraction groups observed from O_2 monolayers at constant filling but at varying temperatures through the $\alpha+\delta$ and $\beta+\delta$ regions of the phase diagram (Fig. 3). The *ZYX* UCAR graphite was used as substrate. The peak at $Q=2.16$ Å^{-1} is a co-existing δ-phase peak. The curves are calculated line shapes assuming a skew triangular structure similar to that shown in Fig. 5(b) for the α phase, but the splitting of the two α phase peaks is varied to obtain the best fit to the observed points.

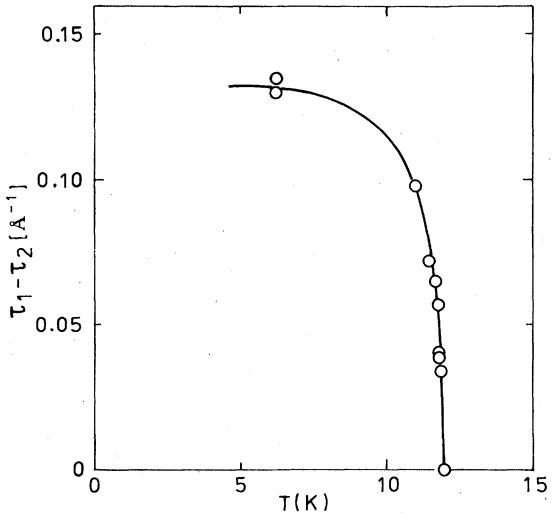

FIG. 13. Splitting of the (10) Bragg peak observed from monolayers of O_2 in the α phase coexisting with O_2 layers of the δ phase. The values of the splitting $\tau_1-\tau_2$ are determined by fitting the curves to the observed points in Fig. 12.

if so, the splitting $\tau_2-\tau_1$ is a measure of the *magnetic* order parameter. The temperature dependence of this splitting is shown in Fig. 13. The sharpness of the transition corresponds to a continuous one with small β (≈ 0.1–0.2), but since the data only go to $\Delta\tau/\Delta\tau(T=0)\approx 0.25$ it is not possible to derive a reliable value. The value of the α–β transition temperature is $T_c = 11.92 \pm 0.08$ °K.

The effect of the second-layer molecules on the α–β transition temperature is small (see Fig. 3). From the change of shape of the nuclear Bragg peaks with increasing occupancy in the second layer (see Fig. 7), we are led to conclude registry between the two layers of O_2 molecules. The natural structure to assume is shown in Fig. 10 but this implies that for coverages between one and two layers a fraction of the first layer must be uncovered and the remaining of the layer covered with the second layer. This gives rise neither to a splitting of the observed Bragg groups, especially significant for the β-phase groups, nor to a smearing of the α-β transition temperature. Therefore, the coupling between the layers must be weak, but still strong enough to ensure registry.

V. DISCUSSION

The α and β phases of monolayer O_2 on graphite bear a close resemblance to the like-designated bulk phases, their structures being essentially those of the closest-packed bulk planes. This is in accordance with the calculations of English, Venables, and Salahub,[1] who discussed the structural and magnetic properties of bulk O_2 in terms of a stack of 2D sheets of O_2 molecules.

It is remarkable that we have observed no effects attributable to the structure or the dynamics of the graphite substrate, other than in its role of providing an adsorption plane. In particular, no commensurate phase was found. This is in contrast to all other systems studied on graphite, with the single exception of argon. It thus seems reasonable to discuss the structures and phase transitions of the O_2 monolayer films in terms of 2D models. As shown by English *et al.*,[1] the equilibrium configuration of a sheet of O_2 molecules would be one in which the molecular centers form

a close-packed equilateral triangular structure, with the molecular axes normal to the plane. This results from maximizing the atom-atom interactions in the presence of a very small quadrupole moment, and neglecting the fluctuations in positions and orientations, as well as magnetic and magnetoeleastic interactions. The monolayer β phase has this predicted structure, but it exists only at temperatures above 11.92 K and for complete monolayer coverages or greater. Presumably, these coverages are needed to prevent the molecules from having large-angle librational fluctuations and perhaps short-range orientational order, which may be present in the as yet ill-characterized submonolayer δ phase.

At temperatures below 11.92 K, magnetic interactions play an essential role in determining the structure of the film. They can be understood in a simple qualitative way in terms of the electronic structure of the isolated O_2 molecule, slightly perturbed by interactions with neighbors. The $^3\Sigma_g^-$ ground state of O_2 has the electronic configuration

$$\sigma_g^2(1s)\sigma_u^{*2}(1s)\sigma_g^2(2s)\sigma_u^{*2}(2s)\sigma_g^2(2p_z)$$

$$\times\pi_u^2(2p_x)\pi_u^2(2p_y)\pi_g^*(2p_x)\pi_g^*(2p_y),$$

and by Hund's rules the two unpaired π^* electrons form a triplet $S=1$ spin state. Two such molecules aligned as in bulk and in 2D O_2 can have extra attractive interactions through virtual low-lying ionic $O_2^- - O_2^+$ states only if, as required by the Pauli principle, their molecular spins S are not parallel. To lowest order, then, there is an additional intermolecular force with effective Hamiltonian of the Heisenberg form

$$E_{12}(r_{12}, \Omega_1, \Omega_2) = |J(r_{12}, \Omega_1, \Omega_2)|(\vec{S}_1 \cdot \vec{S}_2).$$

The exchange integral J is a function of the overlap of the O_2-O_2 molecular orbitals, and thus should depend strongly on intermolecular center of mass distance r_{12}, as well as on molecular orientations Ω_1 and Ω_2.

As a result of this direct exchange interaction pairs of neighboring molecular spins tend to align antiferromagnetically. It is not possible to make such configurations for all nearest neighbors on a triangular lattice, with the result that such a system does not have a well-defined ground state. However, magnetoelastic distortions can produce four nearest neighbors which are antiferromagnetically aligned, the other two ferromagnetic molecules moving out. This also occurs in the closest-packed plane of bulk O_2 below $T=23$ K. Here, and in the monolayer, the four antiferromagnetic neighbors move in approximately 0.1 Å to $a_{\text{n}} \approx 3.20$ Å, while the other two move out to a_{nn} ~3.43 Å. Because of the strong dependence of J on r_{12} it appears that the coupling between these ferromagnetic next-nearest neighbors is insignificant at these distances. In the bulk this situation persists up to the first-order α-β transition at $T=23$ K. For the monolayer system, however, we have observed that both the distortion and the magnetic order are continuous functions of temperature. A complete microscopic 2D model of the system would then require explicit consideration of the dependence of both the intermolecular potential and J on r and Ω, and has not been done to date. Domany and Riedel[8] have, however, examined the properties of a phenomonological Landau-Ginzburg-Wilson Hamiltonian for molecules on an equilateral triangular lattice with antiferromagnetic Heisenberg coupling and cubic anisotropy, together with an elastic distortion term and a magnetoelastic coupling. For the case appropriate to O_2 the magnetic terms cause order, driving the elastic distortion through the coupling terms. In the model this yields a single continuous transition of cubic Heisenberg character, which is predicted to have universal critical exponents.

The continuous nature of this transition is in agreement with our observations, however we can make no definite conclusions on the values of any of the critical exponents, other than to note that β is apparently small. The major difficulty in deriving critical exponents from measurements on adsorbed films stems from the finite coherence length of the 2D layers. The finite size gives rise to a spread of the transition temperature, and this effect dominates the measured results in the critical region even when the ZYX substrate is used.

Recently, Gregory[18] has made magnetic susceptibility measurements of O_2 films on Grafoil. He observed magnetic anomalies in the δ- and β-phase melting regions, but his apparatus did not have sufficient sensitivity to observe the α-β transition. Vilches,[19] however, has seen specific-heat anomalies at all phase boundaries reported in this work, including the α-β one.

The correspondence of the observed α-β transition with that of a 2D system has its limitations, and in particular needs extension in order to discuss the properties of second and higher layers. The pure α phase is not completed until there is a slight second-layer population. However, it comes in at full strength with only a few per cent overfilling, implying that the phase is a monolayer characteristic requiring only the surface pres-

sure provided by the overfilling. It is more difficult, however, to understand the constancy of the transition temperature in the range 1–2 layer. The shape of the α-phase Bragg peaks in this regime as well as the magnetic scattering intensity suggests that the second layer is in registry with the first, and so they must be coupled to some extent, yet we have observed no influence of this on the transition.

The submonolayer δ phase remains a puzzle.

ACKNOWLEDGMENTS

We thank M. Bretz for the permission to use his sample cell containing the *ZYX* UCAR substrate in our study of the α-β structural transition. The research was supported in part by Nato Grant No. 1249 and the research of J. P. McTague was also supported in part by U.S. NSF Grant No. CHE 76-21293.

[1]C. A. English, J. A. Venables, and D. R. Salahub, Proc. R. Soc. Lond. A 340, 81 (1974); C. S. Barret, L. Meyer, and J. Wasserman, J. Chem. Phys. 47, 592 (1967).

[2]C. S. Barret and L. Meyer, Phys. Rev. 160, 694 (1967).

[3]J. P. McTague, M. Nielsen, and L. Passell, CRC Crit. Rev. Solid State Mat. Sci. 8, 135 (1979).

[4]M. D. Chinn and S. C. Fain, Phys. Rev. Lett. 39, 146 (1977); J. A. Venables and P. S. Schabes-Retchkiman, J. Phys. (Paris) Suppl. C 38, 4–105 (1977).

[5]M. Nielsen, W. D. Ellenson, and J. P. McTague, *Neutron Inelastic Scattering* (IAEA, Vienna, 1977), p. 433.

[6]M. Bretz, Phys. Rev. Lett. 38, 501 (1977).

[7]M. Nielsen, J. P. McTague, and W. D. Ellenson, J. Phys. (Paris) Suppl. C 38, 4–10 (1977).

[8]E. Domany and E. K. Riedel, J. Appl. Phys. 49, 1315 (1978); Phys. Rev. Lett. 40, 561 (1978).

[9]Grafoil is the trade name of a pure graphite product which is obtained from Union Carbide Corp., Carbon Product Division, 270 Park Ave., New York, N.Y. 10017.

[10]J. P. McTague and M. Nielsen, Phys. Rev. Lett. 37, 596 (1976).

[11]J. G. Dash, *Films on Solid Surfaces* (Academic, New York, 1976).

[12]J. K. Kjems, L. Passell, H. Taub, J. G. Dash, and A. D. Novaco, Phys. Rev. B 13, 1446 (1976).

[13]M. Nielsen and W. D. Ellenson, in *Proceedings of the Fourteenth International Conference on Low Temperature Physics, Otaniemi, Finland 1975*, edited by M. Krusius and M. Vuorio (North-Holland, Amsterdam, 1975), p. 437.

[14]H. Taub, K. Carneiro, J. K. Kjems, and L. Passell, Phys. Rev. B 16, 4551 (1977).

[15]F. E. Hanson, M. J. Mandell, and J. P. McTague, J. Phys. (Paris) Suppl. C 10, 4–76 (1977).

[16]R. A. Alicanov, I. L. Ilyina, and L. S. Smirnov, Phys. Status Solidi B, 385 (1972).

[17]UCAR *ZYX* is a pure graphite product which can be obtained from Union Carbide Corp., Carbon Product Division, 270 Park Ave., New York, N.Y. 10017.

[18]S. Gregory, Phys. Rev. Lett. 40, 723 (1978).

[19]O. Vilches (unpublished).